New Source of Dislocations in $Ge_xSi_{1-x}/Si(100)$ Strained Epitaxial Layers

D. J. Eaglesham,[(1),(a)] D. M. Maher,[(1,2)] E. P. Kvam,[(1)] J. C. Bean,[(2)] and C. J. Humphreys[(1)]
[(1)] *Department of Materials Science and Engineering, University of Liverpool, P.O. Box 147, Liverpool L69 3BX, United Kingdom*
[(2)] *AT&T Bell Laboratories, 600 Mountain Avenue, Murray Hill, New Jersey 07974*
(Received 9 June 1988)

A new dislocation source has been observed for the first time in Ge_xSi_{1-x}/Si strained epitaxial layers. Transmission electron microscopy reveals that strain relaxation at the "critical thickness" in low-mismatch Ge-Si alloys can occur through the emission of glissile dislocations from $\frac{1}{6}\langle 114\rangle$ stacking faults. A novel mechanism is proposed to explain the observations whereby the $\frac{1}{6}\langle 114\rangle$ boundary dislocation of a stacking fault dissociates (in one of two ways) to emit a $\frac{1}{2}\langle 110\rangle$ glissile dislocation, which then bows out under the applied stress to form a loop. As for a Frank-Read source, closure of the propagating glissile loop regenerates the original extended defect.

PACS numbers: 68.65.+g, 61.16.Di, 61.70.Ga

Dislocation nucleation and multiplication processes in heteroepitaxial semiconductors are subjects of considerable interest (e.g., Refs. 1–23). Experimentally, it is possible to grow essentially dislocation-free epilayers at a significant lattice mismatch to the substrate, provided the epilayer is thinner than some critical thickness t_c (e.g., Refs. 1–5). Further, it appears that for heteroepitaxial semiconductors which are grown layer-by-layer on dislocation-free substrates, t_c is higher than theoretical arguments would predict.[6–14] Thus, as several authors have emphasized,[6–10,15,16] the activation barriers to the nucleation and propagation of dislocations have assumed a central importance to our understanding of this topic. A number of energetic formulations of the dislocation nucleation process have been derived in order to model the breakdown of coherency. However, despite numerous experimental investigations (e.g., Refs. 17–23), no direct evidence has been reported for the introduction of the first misfit dislocations in to a substrate/epilayer materials system free of pre-existing perfect dislocations, and the present work addresses this issue. Studies of the mechanisms by which new dislocations can be introduced into materials can be traced back to the earliest work of dislocation motion during plastic deformation. Frank[24] very early pointed out that there must be a very large activation barrier to the homogeneous nucleation of dislocations. In order to explain plastic deformation in materials with a low dislocation density, a number of dislocation sources were proposed,[25–27] all of which operate through the motion of a pinned perfect-dislocation segment (as opposed to the formation of new dislocations). In the case of certain semiconductor heteroepitaxy systems, however, the density of pre-existing dislocations is thought to be insufficient to provide the necessary relaxation of the epilayer, so that homogeneous nucleation of dislocation half-loops at the surface appears to become the only plausible mechanism.[28,29] Since even at surface steps a minimum misfit of $\sim 2\%$ appears to be required for activation of this process,[29,30] there is a region of lattice mismatch which apparently is too high to be accommodated by the propagation of a reasonably low density of pre-existing dislocations ($\epsilon > 0.1\%$), and too low to activate homogeneous half-loop nucleation processes ($\epsilon < 2\%$). The purpose of this Letter is to address the problem of perfect-dislocation nucleation and multiplication in this region of lattice mismatch.

The breakdown of coherency in $Ga_xSi_{1-x}/Si(100)$ was studied by transmission electron microscopy (TEM) with use of molecular-beam epitaxial layers of fixed thickness but with a graded composition across the wafer; the critical-thickness transition was thus observed as a critical-*misfit* condition. For ~ 180-nm-thick epilayers, the critical misfit occurred at a composition $x \sim 0.13$, corresponding to a critical misfit of $\epsilon_c \sim 0.55\%$ which lies within the region of interest (i.e., $0.1\% \leq \epsilon \leq 2.0\%$). TEM samples were prepared in both cross-section and plan-view geometry by mechanical polishing followed by ion milling (4-kV Ar^+) or chemical thinning (HNO_3-HF). TEM examinations were carried out at 120 and 300 kV predominantly on plan-view specimens in order to observe low dislocation densities.

At compositions very close to ϵ_c and in ~ 180-nm-thick films, the misfit dislocations observed are predominantly 60° type which lie parallel to $\langle 011\rangle$ in the heterointerface and have inclined $\frac{1}{2}\langle 110\rangle$ Burgers vectors. These misfit dislocations are very long (typically 10–100 μm) and they are connected to the growth surface by inclined epithreading screw or 60° dislocation segments lying in the same $\{111\}$ glide plane as the $\langle 011\rangle$ misfit-dislocation segments. A 60° misfit dislocation can propagate down its glide plane to the heterointerface and the length of the misfit-dislocation segment then can increase through the propagation of the epithreading segment under the influence of the epilayer strain, so that once formed these dislocation loops can grow. (Recent TEM observations of the propagation of 60° misfit dislocations during *in situ* heating experiments have confirmed the action of this well-understood process.[16] Coplanar sequences of half-loops on $\{111\}$ dominate the dislocation microstructure in our low-mismatch epilayers

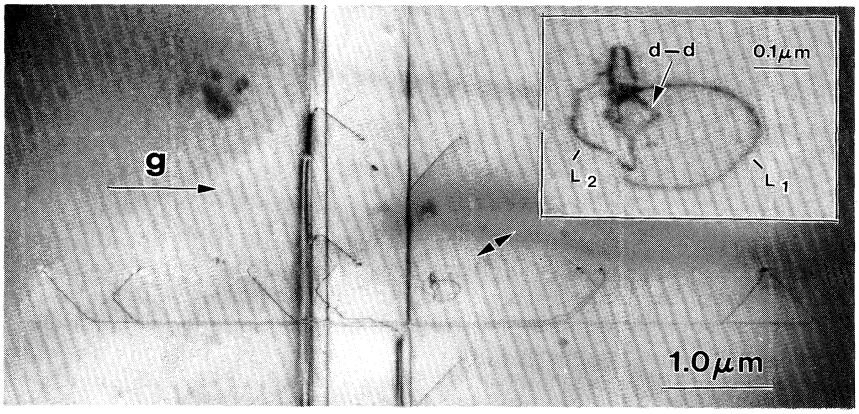

FIG. 1. Bright-field image [recorded near (100) with the 022 reflection excited] showing a sequence of four coplanar glissile half-loops lying on a $(11\bar{1})$ glide plane with mixed Burgers vectors (i.e., $\mathbf{b}=\frac{1}{2}[101]$ and $\mathbf{b}=\frac{1}{2}[1\bar{1}0]$. This microstructure suggests dislocation source action. Inset: A diamond-shaped stacking fault at the center of the innermost half-loop. (Note that the fault is out of contrast in this image, so that only the diamond-shaped boundary dislocation is visible.) This stacking fault (*d-d*) is associated with two glissile dislocation loops: L_1 and L_2 having $\mathbf{b}=\frac{1}{2}[101]$ and $\mathbf{b}_2=\frac{1}{2}[1\bar{1}0]$ and lying on $(11\bar{1})$ and (111), respectively.

(see Fig. 1) and this microstructural feature is indicative of an active dislocation source. A process such as surface nucleation could only account for the geometry of Fig. 1 if nucleation of half-loops was strongly correlated. Detailed diffraction contrast results from the crystal region shown in Fig. 1 reveal that a stacking fault is associated with the smallest (i.e., newly nucleated) dislocation loops (see inset). The stacking fault is diamond shaped, has $\langle 110\rangle$ sides, and lies on the same $\{111\}$ plane as the dislocation loop denoted L_1 which, as shown by stereomicroscopy, is coplanar with the sequence of four half-loops running parallel to the operating reflection, **g**, in Fig. 1. A distribution of diamond defects is observed in all the epilayers studies here and, although the diamond defects are not always associated with dislocations, *all* observed dislocations are associated with a diamond defect which lies close to the $\{111\}$ glide plane of the dislocation. Diffraction contrast analyses of diamond defects have been carried out: The stacking fault (but not the boundary dislocation) is always invisible in one of the 022 reflections normal to the growth direction and both the stacking fault and the boundary dislocation are out of contrast in one of the inclined 311 reflections. These results are consistent with a displacement vector which lies along $\langle 114\rangle$ and a boundary partial dislocation which exhibits strong residual contrast when imaged with a basal-plane 022 reflection. Dynamical image simulations of the residual dislocation contrast in the basal-plane reflection indicate that the most probable Burgers vector for the diamond defect is $\frac{1}{6}\langle 114\rangle$. Thus the defects are apparently similar to those reported in previous studies of faulted defects in silicon (where the defects were attributed to interstitial precipitation in irradiated silicon).[31–33] The diffraction contrast analysis described herein is analogous to that reported in Ref. 32. However, the mechanism for the formation of the diamond defects in Ge-Si heteroepitaxy remains unclear. In what follows, we will explain the way in which the diamond defects are linked to perfect-dislocation nucleation and multiplication in a low-mismatch $Ge_xSi_{1-x}/Si(100)$ system.

In addition to coplanar sequences of half-loops with embryonic dislocation loops still associated with diamond defect (e.g., Fig. 1) we also observe half-loops (i.e., misfit dislocations) which are still attached, in part to a diamond defect (e.g., Fig. 2). There are two other very typical microstructures in which the diamond defect is linked to misfit dislocations (more detailed examples and analyses will be given elsewhere[34]): These involve a diamond defect lying either above a single 60° misfit dislocation or (most characteristically) above an intersection

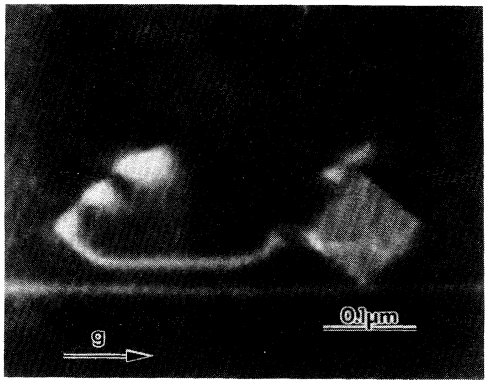

FIG. 2. Dislocation half-loop nucleation in Ge-Si epilayers: weak-beam image of a newly nucleated half-loop attached to a diamond-shaped stacking-fault loop similar to that shown in Fig. 1, suggesting dislocation emission by the diamond defect. Diffraction contrast analysis indicates $\frac{1}{6}\langle 114\rangle$ as the most probable displacement vector for the diamond defect. (022 dark-field image under $g,3g$ weak-beam conditions.)

between two orthogonal bundles of 60° misfit dislocations (e.g., Fig. 3). Moreover, it should be emphasized that the dislocations associated with a single diamond defect very often have different Burgers vectors. Since the density of the diamond defects is not sufficiently high for the observed microstructural features to be explained as coincidences, it seems quite clear that the microstructure is linked to a heterogeneous source and that the operation of this source differs radically from any of those which have been reported previously.

We propose that a $\frac{1}{6}\langle 114\rangle$ partial dislocation which bounds a diamond-shaped stacking fault dissociates by one of the following reactions:

$$\tfrac{1}{6}[114] \rightarrow \tfrac{1}{2}[101] + \tfrac{1}{6}[\bar{2}11]$$

or

$$\tfrac{1}{6}[114] \rightarrow \tfrac{1}{2}[011] + \tfrac{1}{6}[1\bar{2}1].$$

In previous studies, $\frac{1}{6}\langle 114\rangle$ defects have been observed to unfault.[31] The energetics for an unfaulting reaction appear to be more favorable than dissociation: the overall reaction is $\frac{1}{6}[114] + \frac{1}{6}[\bar{1}2\bar{1}] = \frac{1}{2}[011]$ (see Ref. 32). However, the *nucleation* step for the unfaulting reaction must clearly involve the propagation (under the driving force of the stacking-fault energy) of a $\frac{1}{6}\langle 112\rangle$ partial dislocation away from the boundary dislocation which thus becomes $\frac{1}{2}\langle 110\rangle$ (i.e., the initial stages of unfaulting involve precisely the dissociation suggested above). We propose that in a strained materials system, instead of an unfaulting reaction, the glissile $\frac{1}{2}\langle 110\rangle$ dislocation segment may bow out under the epilayer stress to form a half-loop attached to the $\frac{1}{6}\langle 112\rangle$ partial dislocation at each end. The glissile $\frac{1}{2}\langle 110\rangle$ dislocation then closes back onto itself in a manner identical to a Frank-Read source and thereby recombines with the $\frac{1}{6}\langle 112\rangle$ partial dislocation. The final configuration is then the original $\frac{1}{6}\langle 114\rangle$ diamond defect and a $\frac{1}{2}\langle 110\rangle$ dislocation loop propagating outwards on another {111} plane, as shown schematically in Fig. 4. The diamond defect can then emit dislocations repetitively and penetration of the growth surface by $\frac{1}{2}\langle 110\rangle$ dislocation loops results in the coplanar glissile half-loops which are observed experimentally. The crystal region shown in Fig. 2 differs from this normal behavior in that a glissile dislocation loop emitted by the diamond defect is still pinned to the stacking fault, so that the multiplication process is particularly clear. The reason why dissociation occurs, rather than unfaulting, is not yet fully understood: However, strain-relaxation terms must be central to the energetics of a source acting under strain, and may stabilize unfavorable reactions. In addition, the dislocation core energy (unknown for these defects) plays an important part in nucleation.[35]

The microstructure shown in Fig. 3 can now be explained as arising from the different dissociations which can occur at the diamond defect. For any given diamond defect there are two dissociation reactions which must be symmetry equivalent in a tetragonally strained crystal. Thus any individual loop is expected to be able to emit $\frac{1}{2}\langle 110\rangle$ dislocations with two different Burgers vectors. These dislocations will be glissile on the habit plane of the diamond defect, and on one of the two other {111} planes which intersect the boundary dislocations of the diamond defect. While these different planes are not all symmetry identical in their operation, it would be expected that all these modes should be visible in a real materials system. This association of a single diamond defect with half-loops having different Burgers vectors and glide planes has been confirmed by diffraction contrast analyses.[36] Thus the unique source characteristics expected to be associated with the diamond defect are an

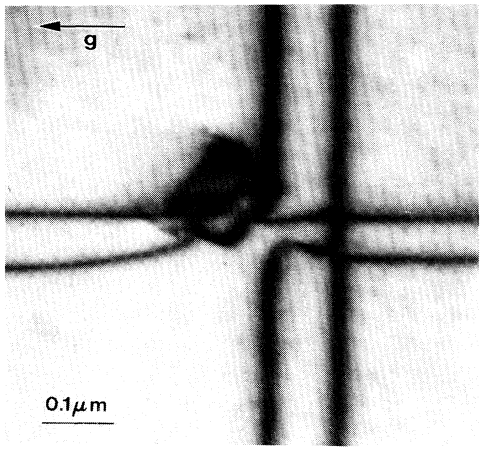

FIG. 3. Dislocation intersection morphology, showing a typical association of the diamond defect with two orthogonal sets of $\frac{1}{2}\langle 110\rangle$ glissile dislocations. Every dislocation in the epilayer is associated with a diamond defect at some such intersection, demonstrating a conclusive link between this defect and the presence of epilayer misfit dislocations. [Bright-field image recorded near (100) with the 022 reflection excited.]

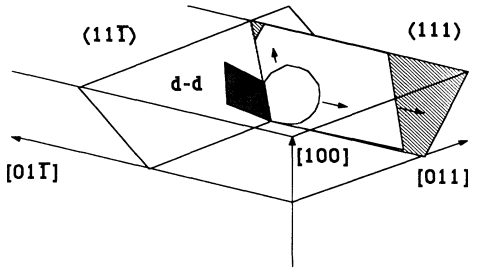

FIG. 4. Schematic diagram of the geometry of the proposed model for dislocation emission by the diamond defect (*d-d*), showing how it can emit a glissile dislocation on a different {111} glide plane. Since the boundary dislocation of the stacking fault loop can dissociate in two distinct ways, dislocation emission by this mechanism can generate sequences with different Burgers vectors on different glide planes, as observed.

orthogonal set of half-loops meeting the heterointerface just below the diamond defect (as in Fig. 3), and the existence of closely grouped sequences of parallel 60° misfit dislocations which have different Burgers vectors (as in Fig. 1). Sequences of coplanar half-loops can be generated by other multiplication mechanisms (e.g., Ref. 18), but the diamond defect is the only source which has been proposed which can generate sequences of dislocation half-loops with different Burgers vectors.

The mechanism we have proposed for dislocation multiplication from the diamond defect will obviously be strain dependent. At thicknesses below the typical size of the diamond defect, this source is clearly unlikely to be operative. Moreover, at higher epitaxial strains, homogeneous nucleation may prevail (e.g., at the largest surface steps which will provide stress concentration effects). Thus the diamond defect is likely to predominate as a source only in a low-lattice-mismatch system. However, the dislocation microstructure generated by this mechanism is probably desirable for epilayer device performance, in that the 60° misfit dislocations are extremely long, so that for a given strain relaxation, the epithreading dislocation density will be low. We have made a comparison between the dislocation microstructure observed in low-misfit ($\epsilon \sim 0.5\%$) and higher-misfit ($\epsilon \sim 2\%$) epilayers (see Ref. 23). The microstructure at higher lattice mismatch is indeed different, with very short edge dislocations dominating. This may be due to the operation of a different nucleation mechanism in the more highly strained epilayers and suggests that the dislocation content in high-misfit epilayers may be reduced by nucleating glissile misfit dislocations at lower Ge content.

In conclusion, we have exposed a novel dislocation source mechanism in low-mismatch Ge-Si epilayers by studying the extended defect microstructure. Misfit dislocations introduced just above the critical thickness and at low lattice mismatch are all observed to be linked to $\frac{1}{6}\langle 114\rangle$ stacking faults. The observed microstructure is shown to be consistent with dislocation emission from these "diamond defects." This operation of the diamond defect via a dissociation reaction represents the first observation of a completely new type of dislocation source. This source depends on the presence of the diamond defect (which we observe in all epilayers studied here) and on certain compositional requirements: A composition-dependent microstructure is indeed observed. This in turn suggests a method for reducing the threading dislocation density in relaxed Ge-Si epitaxial layers.

---

[a]Now at AT&T Bell Laboratories, 600 Mountain Avenue, Murray Hill, NJ 07974.

[1]J. C. Bean, L. C. Feldman, A. T. Fiory, S. Nakahara, and I. J. Robinson, J. Vac. Sci. Technol. A **2**, 436 (1984).

[2]A. T. Fiory, J. C. Bean, L. C. Feldman, and I. K. Robinson, J. Appl. Phys. **56**, 1227 (1984).

[3]A. T. Fiory, J. C. Bean, R. Hull, and S. Nakahara, Phys. Rev. B **31**, 4063 (1985).

[4]E. Kasper and H.-J. Herzog Thin Solid Films **44**, 357 (1977).

[5]Y. Kuk, L. C. Feldman, and P. J. Silverman, Phys. Rev. Lett. **50**, 511 (1983).

[6]J. H. Van der Merwe, J. Appl. Phys. **34**, 123 (1963).

[7]R. People, IEEE J. Quantum Electron. **22**, 1696 (1986).

[8]B. W. Dodson and J. Y Tsao, Appl. Phys. Lett. **51**, 1325 (1987).

[9]B. W. Dodson, Proc. Mater. Res. Soc. **116**, 491 (1988).

[10]J. Naryan, S. Sharan, A. R. Srivatsa, and A. S. Nandedkar, Mater. Sci. Eng. B **1**, 105 (1988).

[11]R. People and J. C. Bean, Appl. Phys. Lett. **47**, 322 (1985).

[12]R. People and J. C. Bean, Appl. Phys. Lett. **49**, 229 (1986).

[13]M. Grabow and G. Gilmer, Proc. Mater. Res. Soc. **94**, 15 (1987).

[14]M. Grabow and G. Gilmer, Proc. Mater. Res. Soc. **103**, 13 (1988).

[15]P. M. J. Marée, J. C. Barbour, J. F. Van der Veen, K. L. Kavanaugh, C. W. T. Bulle-Lieuwana, and M. P. A. Viegers, J. Appl. Phys. **62**, 4413 (1987).

[16]R. Hull, J. C. Bean, D. J. Warder, and R. E. Leibenguth, Appl. Phys. Lett. **52**, 1605 (1988).

[17]J. P. Petroff, M. Sauvage, and Lure, J. Cryst. Growth **43**, 628 (1978).

[18]W. Hagen and H. Strunk, Appl. Phys. **17**, 85 (1978).

[19]H. Strunk, W. Hagen, and E. Bauser, Appl. Phys. **18**, 67 (1979).

[20]E. P. Kvam, D. J. Eaglesham, C. J. Humphreys, D. M. Maher, J. C. Bean, and H. L. Fraser, in *Microscopy of Semiconducting Materials 1987,* edited by A. G. Cullis, IOP Conference Proceedings No. 87 (Institute of Physics, London, 1987), p. 165.

[21]I. J. Fritz, Appl. Phys. Lett. **51**, 1080 (1987).

[22]K. Rajan and M. Denhoff, J. Appl. Phys. **62**, 1710 (1987).

[23]E. P. Kvam, D. J. Eaglesham, D. M. Maher, and C. J. Humphreys, J. C. Bean, G. S. Green, and B. Tanner, Proc. Mater. Res. Soc. **104**, 623 (1988).

[24]F. C. Frank, in *Symposium on Plastic Deformation of Crystalline Solids* (Carnegie Institute of Technology Pittsburgh, 1950), p. 89.

[25]F. C. Frank and W. T. Read, in Ref. 24, p.44.

[26]J. S. Koehler, Phys. Rev. **86**, 52 (1952).

[27]F. R. N. Nabarro, in *Report of the Conference on Strength of Solids* (Physical Society, London, 1949), p. 75.

[28]J. P. Hirth, in *Relation Between Structure and Strength in Metals and Alloys* (Her Majesty's Stationary Office, London, 1963), p. 218.

[29]J. W. Matthews, J. Vac. Sci. Technol. **12**, 126 (1975).

[30]J. W. Matthews, A. E. Blakeslee, and S. Mader, Thin Solid Films **33**, 253 (1976).

[31]J. Grilhe, K. Seshan, and J. Washburn, Radiat. Eff. **27**, 155 (1975).

[32]J. A. Lambert and P. S. Dobson, Philos. Mag. A **37**, 441 (1978).

[33]I. G. Salisbury, Acta Metall. **30**, 627 (1982).

[34]D. J. Eaglesham, E. P. Kvam, D. M. Maher, C. J. Humphreys, and J. C. Bean, Philos. Mag. (to be published).

[35]A. S. Nandedkar and J. Narayan, Philos. Mag. A **56**, 625 (1987).

[36]D. J. Eaglesham and D. M. Maher, unpublished.

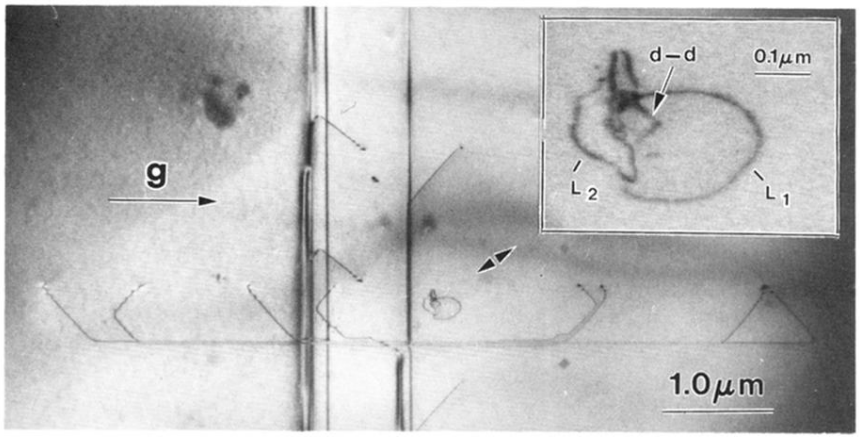

FIG. 1. Bright-field image [recorded near (100) with the 022 reflection excited] showing a sequence of four coplanar glissile half-loops lying on a $(11\bar{1})$ glide plane with mixed Burgers vectors (i.e., $\mathbf{b} = \frac{1}{2}[101]$ and $\mathbf{b} = \frac{1}{2}[1\bar{1}0]$. This microstructure suggests dislocation source action. Inset: A diamond-shaped stacking fault at the center of the innermost half-loop. (Note that the fault is out of contrast in this image, so that only the diamond-shaped boundary dislocation is visible.) This stacking fault (*d-d*) is associated with two glissile dislocation loops: L_1 and L_2 having $\mathbf{b} = \frac{1}{2}[101]$ and $\mathbf{b}_2 = \frac{1}{2}[1\bar{1}0]$ and lying on $(11\bar{1})$ and (111), respectively.

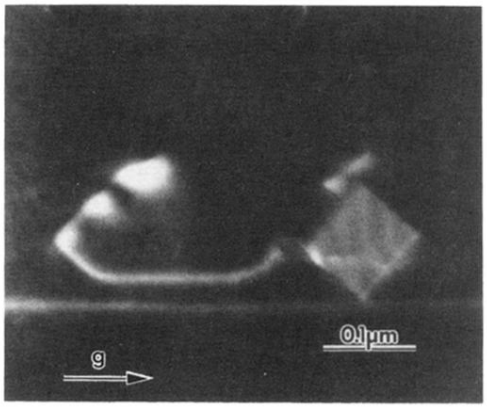

FIG. 2. Dislocation half-loop nucleation in Ge-Si epilayers: weak-beam image of a newly nucleated half-loop attached to a diamond-shaped stacking-fault loop similar to that shown in Fig. 1, suggesting dislocation emission by the diamond defect. Diffraction contrast analysis indicates $\frac{1}{6}\langle 114\rangle$ as the most probable displacement vector for the diamond defect. (022 dark-field image under $g,3g$ weak-beam conditions.)

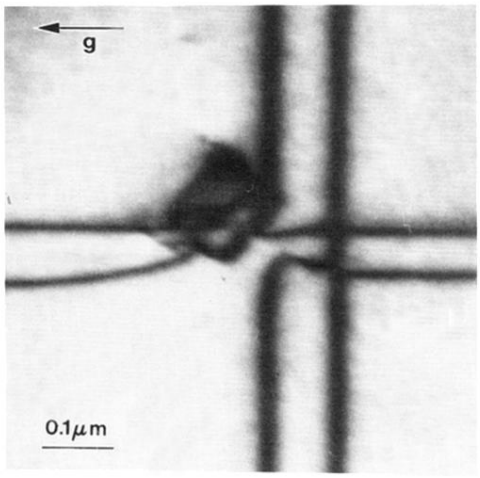

FIG. 3. Dislocation intersection morphology, showing a typical association of the diamond defect with two orthogonal sets of $\frac{1}{2}\langle 110\rangle$ glissile dislocations. Every dislocation in the epilayer is associated with a diamond defect at some such intersection, demonstrating a conclusive link between this defect and the presence of epilayer misfit dislocations. [Bright-field image recorded near (100) with the 022 reflection excited.]